

Quantized Hodgkin-Huxley Model for Quantum Neurons

Tasio Gonzalez-Raya,¹ Xiao-Hang Cheng,² Iñigo L. Egusquiza,³ Xi Chen,² Mikel Sanz,^{1,*} and Enrique Solano^{2,1,4}

¹*Department of Physical Chemistry, University of the Basque Country UPV/EHU, Apartado 644, 48080 Bilbao, Spain*

²*Department of Physics, Shanghai University, 200444 Shanghai, China*

³*Department of Theoretical Physics and History of Science,*

University of the Basque Country UPV/EHU, Apartado 644, 48080 Bilbao, Spain

⁴*IKERBASQUE, Basque Foundation for Science, Maria Diaz de Haro 3, 48013 Bilbao, Spain*

The Hodgkin-Huxley model describes the behavior of the membrane voltage in neurons, treating each element of the cell membrane as an electric circuit element, namely capacitors, memristors and voltage sources. We focus on the activation channel of potassium ions, since it is simpler, while keeping the majority of the features identified with the original Hodgkin-Huxley model. This reduces to a memristor, a resistor whose resistance depends on the history of electric signals that have crossed it, coupled to a voltage source and a capacitor. Here, we take advantage of the recent quantization of the memristor to look into the Hodgkin-Huxley model in the quantum regime. We compare the behavior of the membrane voltage and the potassium channel conductance in both the classical and quantum realms, subjected to AC sources. Numerical simulations show an expected increment and adaptation depending on the history of signals in all regimes. We find that the response of this circuit can be reproduced classically; however, when computing higher moments of the voltage, we encounter purely quantum terms related to the zero-point energy of the circuit. This result paves the way for the construction of quantum neuron networks inspired in the brain function but capable of dealing with quantum information. This could be considered a step forward towards the design of neuromorphic quantum architectures with direct applications in quantum machine learning.

I. INTRODUCTION

Brain science and neurophysiology are fascinating topics with deep questions and implications in the comprehension of the human being. Understanding how the brain works and the desire to use this knowledge to improve our lives catalyzed interdisciplinary research fields such as biophysics and bioinformatics. In 1963, the Nobel Prize in Physiology or Medicine was awarded to Alan Lloyd Hodgkin and Andrew Fielding Huxley for their work describing how electric signals in neurons propagate through the axon. This work consists on modelling small segments of the axon membrane as an electric circuit represented by a set of non-linear differential equations [1], establishing a bridge between neuroscience and physics. Numerous researches about Hodgkin-Huxley's neuron including noise sources have been published [2–9].

A neuron is an electrically excitable cell that receives, processes and transmits information through electrical signals, whose main components are the cell body, the dendrites and the axon. Dendrites are ramifications which receive and transmit stimulus into the cell body, which processes the signal. The nervous impulse is then propagated through the axon, which is an extension of the nerve cell. This propagation gradient is generated through the change in the ion permeabilities of the cell membrane when an impulse is transmitted. This implies a variation in ion concentrations represented in

the Hodgkin-Huxley circuit by a non-linear conductance whose resistance depends on the history of electric charges crossing the cell, which is naturally identified with a memristor [10, 11].

In the last decade, we have witnessed a blossoming of quantum platforms and technologies. From the latter, Quantum Simulations, Quantum Detection and Quantum Communication are worth mentioning. Among quantum platforms, superconducting circuits stand out and currently show the highest gradient in controllability, scalability and coherence. The combination of biosciences with quantum technologies from different perspectives gave rise to new research areas such as quantum biology [12, 13], quantum artificial life [14, 15] and quantum biomimetics [16], among others. In this framework, the merge of neurosciences and quantum technologies has also been considered, resulting, for instance, in the novel concept of neuromorphic quantum computing, in which brain-inspired architectures strive to take advantage of entanglement to enhance computational power.

The recent proposal of techniques for the quantization of the memristor [17], as well as its realization in both superconducting circuits [18] and integrated quantum photonics [19], allows for the construction of a quantized neuron model based on Hodgkin-Huxley's circuit. In the classical limit, this model reproduces the characteristic adaptive behavior of brain neurons, whereas in the quantum regime it could unveil unique characteristics or an unprecedented learning performance. Furthermore, the study of coupled electric circuits

* mikel.sanz@ehu.eus

containing memristors developed in recent years [20–22] sets an excellent starting position for the investigation of the dynamics of coupled quantum memristors for the construction of connected quantum neuron networks.

The idea of proposing mathematical models which condense the main features of real neurons is an old research area, and an attempt to extend it to the quantum realm has been launched in the recent past [23–28]. Furthermore, classical memristive devices have been used in the simulation of synaptic [29–31] as well as learning processes [32]. However, none of those works ever considered the Hodgkin-Huxley model with the quantum memristor.

In this article, we study a simplified version of the Hodgkin-Huxley model with biological interest, in which only the potassium ion channel plays a role. The ion channel conductance, modelled by a memristor, is coupled to a voltage source and a capacitor, and we study its response under a periodic driving in both the classical and quantum regimes. Introducing a quantum memristor [17], we investigate the quantum regime by quantizing the elements in this circuit, comparing the membrane voltage, the conductance and the I-V characteristic curve for different input sources [33]. This work establishes a roadmap for the construction of hardware-based quantum neuron networks, and the application to neuromorphic quantum architectures and quantum neural networks [34]. This could find applications in the field of quantum machine learning [35, 36] without the necessity of a universal quantum computer.

II. CLASSICAL HODGKIN-HUXLEY MODEL

The cell membrane of a neuron shows permeability changes for different ion species after receiving electric impulses through the dendrites. These changes make possible variations on ion concentrations which, when a certain threshold is overcome, can lead to a sudden depolarization of the membrane and the consequent transmission of the signal through the axon. These ions comprise mainly potassium and sodium, which have different roles

during a potential spike. In 1952, Hodgkin and Huxley developed a model which describes the propagation of these stimuli by treating each component of the excitable cell membrane as an electric circuit element, as shown in Fig. 1 (a). The equations of this circuit are

$$I(t) = C_g \frac{dV_g}{dt} + \bar{g}_K n^4 (V_g - V_K) + \bar{g}_{N_a} m^3 h (V_g - V_{N_a}) + \bar{g}_L (V_g - V_L), \quad (1)$$

$$\frac{dn}{dt} = \alpha_n(V_g)(1 - n) - \beta_n(V_g)n, \quad (2)$$

$$\frac{dm}{dt} = \alpha_m(V_g)(1 - m) - \beta_m(V_g)m, \quad (3)$$

$$\frac{dh}{dt} = \alpha_h(V_g)(1 - h) - \beta_h(V_g)h, \quad (4)$$

where I is the total current, \bar{g}_i ($i = L, K, N_a$) are constants representing the maximum value each electrical conductance can take, C_g is the membrane capacitance, V_i is the resting potential in each ion channel, and n, m , and h are dimensionless quantities between 0 and 1 that represent the probability of activation or inactivation of each ion channel. Except for the leakage channel L , which accounts for small unperturbed flow of non-involved (mostly chloride) ions, and thus is described by a constant conductance, any ion channel is characterized by a non-linear conductance due to n, m and h , which weigh each channel differently and depend on voltage and time. Here, we keep solely the contribution coming from the potassium channel, which only has activation gates, and not both activation and inactivation gates as the sodium channel. This model still conserves the most characteristic behavior of neurons. In this case, we are left with two coupled differential equations,

$$I(t) = C_g \frac{dV_g}{dt} + g_K n^4 (V_g - V_K), \quad (5)$$

$$\frac{dn}{dt} = \alpha_n(V_g)(1 - n) - \beta_n(V_g)n. \quad (6)$$

Naturally, this non-linear conductance can be identified with a memristor, which is a resistor whose resistance depends on the history of electrical signals, voltages or charges, that have crossed it [10]. It is the fourth basic element of electrical circuits, and introduces a relation between flux and charge. The equations describing the physical properties and memory effects of a (voltage-controlled) memristor are

$$I(t) = G(\mu(t))V(t), \quad (7)$$

$$\dot{\mu}(t) = f(\mu(t), V(t)), \quad (8)$$

where $G(\cdot)$ and $f(\cdot)$ are continuous real functions satisfying:

- (i) $G(\mu) \geq 0$ for all values of μ .
- (ii) For a fixed μ , $f(\mu, V)$ is monotone, and $f(\mu, 0) = 0$.

Property (i) means that $G(\mu)$ can indeed be understood as a conductance, so that Eq. 7 can be interpreted

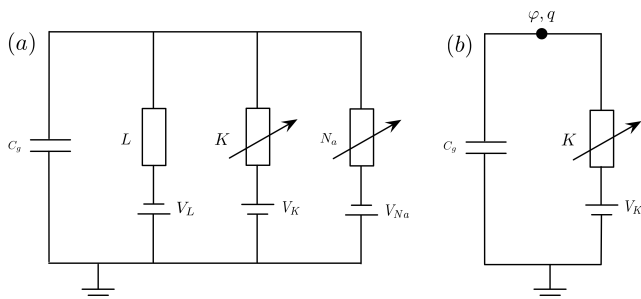


FIG. 1. (a) Complete Hodgkin-Huxley circuit and (b) Hodgkin-Huxley circuit with solely a potassium ion channel.

as a state-dependent Ohm's law. This ensures that the memristor is a passive element. Property (ii) restricts the internal variable dynamics to provide non-vanishing memory effects for all significant voltage inputs, implying that it does not have dynamics in the absence of voltage.

Notice that solving Eq. 8 requires time integration over the past of the control signal, and this solution affects $G(\mu)$. This means that the response in the current given by Eq. 7 depends not only on the present value of the control voltage, but also on the previous ones. Hence, if a memristor undergoes a periodic control signal, the I-V characteristic curve will display a hysteresis loop, which contains memory effects, identifying the slope of this curve with the resistance of the device.

The study of a single ion channel means neutralizing the dynamics of the other channel, which is a matter of controlling its voltage, namely its ionic concentration. Experimentally, an isolated study of the potassium channel is achieved by setting the membrane voltage to V_{Na} , or through changing the sodium concentration by replacing the sodic medium by any other non-gated substance. This was performed in Ref. [1], and allowed them to obtain experimental results that could be compared to theoretical ones, thus testing the proposed expressions for α_x and β_x , with $x = n, m, h$ separately for each channel, so that values for n, m, h could be obtained. Then, with the conductance of the potassium channel given by $g_K = \bar{g}_K n^4$, Eqs. 5 and 6 can be solved numerically for the membrane voltage, given an input current $I(t)$.

III. QUANTUM HODGKIN-HUXLEY MODEL

In this section, we introduce a quantum version of the Hodgkin-Huxley model by quantizing each element of the circuit with one non-linear resistor, a voltage source and two capacitances. First, let us introduce the quantization of the memristor [17].

A. Quantum Memristor

We give a general description of the quantum memristor as a non-linear element in a closed circuit with a weak-measurement scheme, used to update the resistance. This layout can be seen in Fig. 2 as a closed system coupled to a resistor and a measurement apparatus, introducing a measurement-based update of the resistance depending on the voltage in the system.

The dynamics of the composite system can be studied by a master equation composed of a Hamiltonian part, a continuous-weak-measurement part and a classical feedback part,

$$d\rho = d\rho_H + d\rho_m + d\rho_d. \quad (9)$$

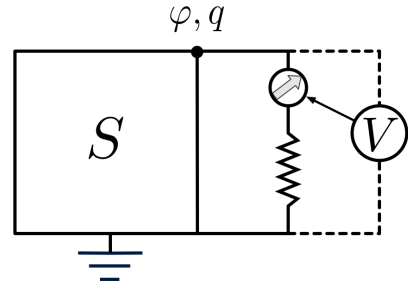


FIG. 2. Diagram of a quantum memristor as a resistor coupled to a closed system with a voltage-based weak-measurement scheme.

The Hamiltonian part is given by the von Neumann equation,

$$d\rho_H = -\frac{i}{\hbar}[H_S, \rho(t)]dt. \quad (10)$$

The continuous-weak-measurement part reads

$$d\rho_m = -\frac{\tau}{q_0^2}[q, [q, \rho(t)]]dt + \sqrt{\frac{2\tau}{q_0^2}}(\{q, \rho(t)\} - 2\langle q \rangle \rho(t))dW, \quad (11)$$

where $[\cdot, \cdot]$ denotes the commutator and $\{\cdot, \cdot\}$ the anti-commutator. The expectation value of an observable is $\langle A \rangle = \text{tr}(\rho A)$, τ is the projection frequency, q_0 is the uncertainty, and dW is the Wiener increment, associated to the stochasticity associated with weak measurements. The measurement strength is defined as $\kappa = \frac{\tau}{q_0^2}$.

The dissipation is described by Caldeira-Leggett master equation,

$$d\rho_d = -\frac{i\gamma(\mu)}{\hbar}[\varphi, \{q, \rho(t)\}]dt - \frac{2C\lambda\gamma(\mu)}{\hbar}[\varphi, [\varphi, \rho(t)]]dt \quad (12)$$

where $\lambda = k_B T / \hbar$ and $\gamma(\mu)$ is the relaxation rate. Solving these equations we can have the relation between memristive current and the charge shown in Fig. 3, for an LC circuit coupled to a memristor, with a Hamiltonian of the form $H_S = \frac{q^2}{2C} + \frac{\phi^2}{2L}$. We can observe that the memristor starts to show linearity in the hysteresis curves as we increase the voltage. In the case of a circuit with classical sources, or a circuit coupled to an open element, there is no need to introduce the Wiener noise.

B. Circuit Quantization

We now proceed to study the quantization of the circuit shown in Fig. 4, for which we must obtain the Lagrangian. With a Hamiltonian formulation on sight, a description of electric circuits entails defining fluxes and charges, from which the voltage and the current can be obtained by time differentiation. In this case we employ

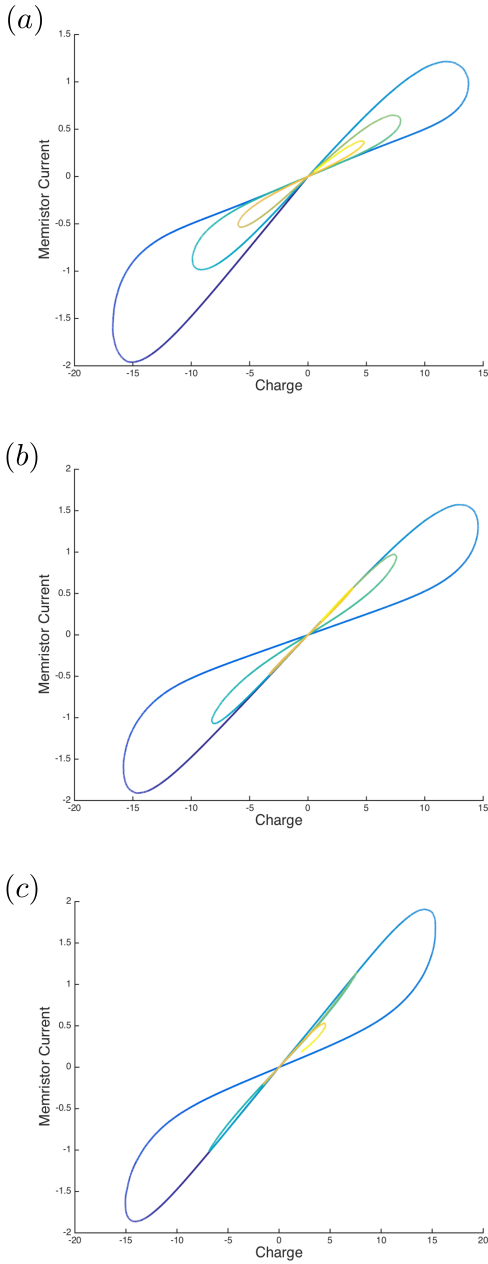


FIG. 3. Hysteresis loops a quantum memristor coupled to a LC circuit with a system Hamiltonian $H_S = \frac{q^2}{2C} + \frac{\phi^2}{2L}$, with $C = 1$ and $L = 1$ for different values of the voltage source: (a) $V = 0$, (b) $V = 1$, (c) $V = 2$

a node formulation, where node fluxes are the main variables and play the role of the spatial variable, with node charges being the conjugate variables. This formulation with node fluxes suffices to describe a circuit featuring linear capacitances and inductances.

Although in the Lagrangian formalism dissipative elements such as resistors can be treated by the addition of a dissipation function to the equations of motion of

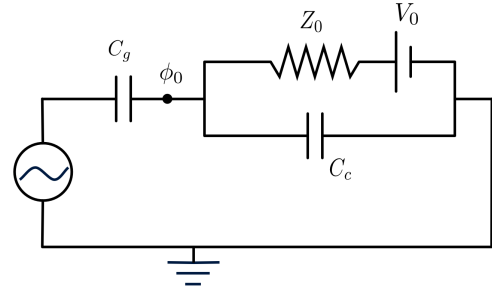


FIG. 4. Hodgkin-Huxley circuit for a single ion channel with a classical AC source $I(t) = I_0 \sin(\Omega t)$, where C_g is the capacitance coupling the source to the circuit, C_c accounts for the axon's membrane capacitance, V_0 is the resting potential for the potassium ion channel, and Z_0 is the resistance of the memristor.

an effective Lagrangian [37], the reversibility of Hamilton's equations, arising from a Hamiltonian formulation needed for a proper circuit quantization, conflicts with the irreversibility of dissipative terms. A solution to this problem is to assume linear dissipation and treat the dissipative element in the Caldeira-Leggett model [38]. In this context, we replace a linear dissipative element by an infinite set of coupled LC oscillators with a frequency-dependent impedance $Z(\omega)$, i.e. a transmission line. The now infinite degrees of freedom of the resistor are identified with the intermediate node fluxes of the oscillators. This way we introduce the memristor as a linear dissipative element cast in the Caldeira-Leggett model.

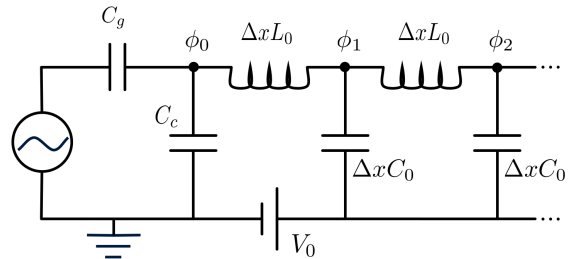


FIG. 5. Hodgkin-Huxley circuit for a single ion channel with a classical AC source $I(t) = I_0 \sin(\Omega t)$ effectively coupled to a semi-infinite transmission line. C_0 and L_0 are the capacitance and inductance corresponding to the transmission line, C_g is the capacitance coupling the source to the circuit, C_c accounts for the axon's membrane capacitance, and V_0 is the resting potential for the potassium ion channel.

The circuit can be seen in Fig. 5. We identify the impedance of the transmission line with the resistance of the memristor, and assuming that the time between consecutive updates is much larger than the relaxation time of the memristor, the impedance can be updated.

The Lagrangian of this circuit is

$$\mathcal{L} = \frac{C_g}{2}(\dot{\phi}_0 - \dot{\phi}_s)^2 + \frac{C_c}{2}\dot{\phi}_0^2 - \frac{(\phi_1 - \phi_0)^2}{2\Delta x L_0} + \sum_{i=1}^{\infty} \left[\frac{\Delta x C_0}{2}(\dot{\phi}_i - V_0)^2 - \frac{(\phi_{i+1} - \phi_i)^2}{2\Delta x L_0} \right], \quad (13)$$

with C_0 and L_0 the characteristic capacitance and impedance per unit length of the transmission line, and the classical current source defined as $I(t) = -C_g(\dot{\phi}_0 - \dot{\phi}_s)$. The equations of motion for this circuit can be obtained as Euler-Lagrange equations, $\frac{d}{dt} \frac{\partial \mathcal{L}}{\partial \dot{\phi}} = \frac{\partial \mathcal{L}}{\partial \phi}$. For the intermediate node fluxes on the transmission line, ϕ_i , we find

$$\ddot{\phi}_i = \frac{1}{L_0 C_0} \frac{\partial^2 \phi_i}{\partial x^2} \quad (14)$$

after taking the continuum limit, $\Delta x \rightarrow 0$, and this is the wave equation for a flux field at position x_i on the transmission line. The general solution to this equation can be written in terms of ingoing and outgoing waves, $\phi(x, t) = \phi_{\text{in}}(t + x/v) + \phi_{\text{out}}(t - x/v)$, with velocity $v = 1/\sqrt{L_0 C_0}$. This leads to the relations

$$\begin{aligned} \frac{\partial \phi(x, t)}{\partial t} &= \dot{\phi}_{\text{in}}(t + x/v) + \dot{\phi}_{\text{out}}(t - x/v), \\ \frac{\partial \phi(x, t)}{\partial x} &= \frac{1}{v}(\dot{\phi}_{\text{in}}(t + x/v) - \dot{\phi}_{\text{out}}(t - x/v)), \end{aligned} \quad (15)$$

which allows us to obtain $\frac{\partial \phi_0(t)}{\partial x} = \frac{1}{v}(2\dot{\phi}_{\text{in}}(t) - \dot{\phi}_0(t))$. The voltage in the circuit can be obtained as $\langle \dot{\phi}_0(t) \rangle$, and the equation for ϕ_0 is

$$-I(t) + C_c \ddot{\phi}_0 = \frac{1}{L_0} \frac{\partial \phi_0}{\partial x} \quad (16)$$

having taken the continuum limit, and identifying $\phi_0(t)$ with $\phi(x=0, t)$, the flux field inside the transmission line at $x=0$. We use this to rewrite the equation of motion for ϕ_0 ,

$$-I(t) + C_c \ddot{\phi}_0 + \frac{\dot{\phi}_0}{Z_0} = 2 \frac{\dot{\phi}_0^{\text{in}}}{Z_0}, \quad (17)$$

where $Z_0 = \sqrt{L_0/C_0}$ is the impedance of the transmission line. The flux field on a semi-infinite transmission line can be written in terms of ingoing and outgoing modes which satisfy canonical commutation relations. The quantization of this field has been performed, for example in Ref. [40], for infinite electrical networks.

As a starting point, we write the decomposition

$$\phi(x, t) = \sqrt{\frac{\hbar Z_0}{4\pi}} \int_0^\infty \frac{d\omega}{\sqrt{\omega}} (a_{\text{in}}(\omega) e^{i(k_\omega x - \omega t)} + a_{\text{out}}(\omega) e^{-i(k_\omega x + \omega t)} + \text{h.c.}), \quad (18)$$

where $k_\omega = |\omega| \sqrt{L_0 C_0}$ is the wave vector and $Z_0 = \sqrt{L_0/C_0}$ is the characteristic impedance of the transmission line, associated with the resistance of the memristor. Since $a_{\text{in}}(\omega)$ and $a_{\text{out}}(\omega)$ can be promoted to quantum operators, $\phi_0(t)$ is promoted to a quantum operator. By combining Eq. 17 with Eq. 18 and writing the Fourier transform of the current, $I(t) = \int_0^\infty \frac{d\omega}{\sqrt{\omega}} (\mathcal{I}(\omega) e^{-i\omega t} + \mathcal{I}^*(\omega) e^{i\omega t})$, we can express the outgoing modes in terms of the ingoing ones,

$$a_{\text{out}}(\omega) = a_{\text{in}}(\omega) \frac{i - C_c \omega Z_0}{i + C_c \omega Z_0} - \frac{1}{\omega} \sqrt{\frac{4\pi Z_0}{\hbar}} \frac{\mathcal{I}(\omega)}{i + C_c \omega Z_0}, \quad (19)$$

with a source term, where $R(\omega) = \frac{i - C_c \omega Z_0}{i + C_c \omega Z_0}$ is the reflection coefficient, and we identify $s(\omega) = \frac{1}{\omega} \sqrt{\frac{4\pi Z_0}{\hbar}} \frac{\mathcal{I}(\omega)}{i + C_c \omega Z_0}$, with $\mathcal{I}(\omega) = \frac{\sqrt{\omega}}{2\pi} \int_{-\infty}^\infty dt e^{i\omega t} I(t)$. Then the voltage in the circuit is

$$\begin{aligned} \langle \dot{\phi}_0(t) \rangle &= -i \sqrt{\frac{\hbar Z_0}{4\pi}} \int_0^\infty d\omega \sqrt{\omega} \left[\left(\langle a_{\text{in}}(\omega) \rangle (1 + R(\omega)) \right. \right. \\ &\quad \left. \left. - s(\omega) \right) e^{-i\omega t} - \text{h.c.} \right]. \end{aligned} \quad (20)$$

By choosing the state of the transmission line to be the vacuum, $\langle 0 | a_{\text{in}}(\omega) | 0 \rangle = \langle 0 | a_{\text{in}}^\dagger(\omega) | 0 \rangle = 0$, we find the voltage in the circuit to be

$$\begin{aligned} \langle \dot{\phi}_0 \rangle &= Z_0 \int_0^\infty \frac{d\omega}{\sqrt{\omega}} \left[\frac{\mathcal{I}(\omega) e^{-i\omega t} + \mathcal{I}^*(\omega) e^{i\omega t}}{1 + (C_c \omega Z_0)^2} \right. \\ &\quad \left. + i C_c \omega Z_0 \frac{\mathcal{I}(\omega) e^{-i\omega t} - \mathcal{I}^*(\omega) e^{i\omega t}}{1 + (C_c \omega Z_0)^2} \right]. \end{aligned} \quad (21)$$

For a classical input current $I(t) = I_0 \sin(\Omega t)$ we have $\mathcal{I}(\omega) = \frac{i I_0 \sqrt{\omega}}{2} (\delta(\omega - \Omega) - \delta(\omega + \Omega))$, for which the voltage response of the system is

$$\langle \dot{\phi}_0 \rangle = I_0 Z_0 \frac{\sin(\Omega t) - C_c \Omega Z_0 \cos(\Omega t)}{1 + (C_c \Omega Z_0)^2}. \quad (22)$$

Actually, this is what is obtained when studying the stationary solution of Eq. 17 with $\dot{\phi}_0^{\text{in}} = 0$. Claiming that ϕ_0 is a valid quantum operator, we compute the second moment of the voltage,

$$\langle \dot{\phi}_0^2 \rangle = \frac{\hbar Z_0}{\pi} \int_0^\infty d\omega \frac{\omega}{1 + (C_c \omega Z_0)^2} + \left[Z_0 \int_0^\infty \frac{d\omega}{\sqrt{\omega}} \frac{\mathcal{I}(\omega) e^{-i\omega t} + \mathcal{I}^*(\omega) e^{i\omega t} + i C_c \omega Z_0 (\mathcal{I}(\omega) e^{-i\omega t} - \mathcal{I}^*(\omega) e^{i\omega t})}{1 + (C_c \omega Z_0)^2} \right]^2. \quad (23)$$

The second term gives the voltage squared, so it has a classical origin, but the first term is purely quantum. It is related to the reflection of the modes in the circuit, and gives the zero-point energy. It diverges as $\omega \rightarrow \infty$, which is a purely quantum mechanical result [38]. This proves that we are dealing with a quantum operator.

In order to observe memristive behavior of the system, we proceed by introducing the update of the resistance of the memristor, considering the dependence of Z_0 on the circuit voltage. This approach is valid as long as the relaxation time of the set of LC oscillators which represents the instantaneous resistor is much shorter than the time scale associated to the change in the resistance. This is equivalent to an adiabatic approximation [39], in which we consider Z_0 constant to obtain the value of the circuit voltage, which we afterwards use to consistently update Z_0 . In this process, we assume that it changes slowly in comparison with the relaxation time of the circuit. Identifying the inverse of the impedance (known as admittance) with a conductance, we can use the equation $g_K(t) = \bar{g}_K n(t)^4$ of the potassium channel conductance to update the impedance as $Z(t) = Z_{\min} n(t)^{-4}$, using Eq. 6, such that

$$\dot{Z}(t) = -4Z_{\min} \left(\frac{Z(t)}{Z_{\min}} \right)^{5/4} \alpha(V_g) + 4Z(t) \left(\alpha(V_g) + \beta(V_g) \right), \quad (24)$$

Thus, from now on, we identify the potassium channel conductance with the inverse of the impedance of the transmission line. Notice that, in this treatment, we have assumed that the voltage measurements used to update the impedance of the memristor do not perturb the system, considering measurements in this setup to be automatic and non-invasive.

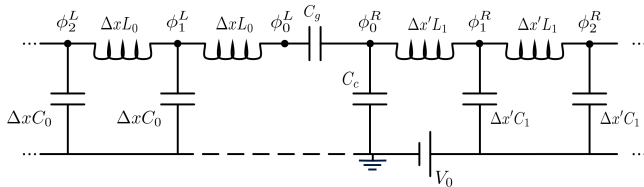


FIG. 6. Hodgkin-Huxley circuit for a single ion channel coupled to a semi-infinite transmission line, introducing a quantized source on the left modelled by a second semi-infinite transmission line. C_0 and L_0 are the capacitance and inductance corresponding to the left transmission line, and the ones corresponding to the right transmission line are C_1 and L_1 . C_g is the capacitance coupling both transmission lines, C_c accounts for the axon's membrane capacitance, and V_0 is the resting potential for the potassium ion channel.

To study the response of this circuit to quantum state inputs, we replace the source with a second semi-

infinite transmission line, thus introducing a collection of LC circuits in which multiple frequencies can be excited. This circuit is depicted in Fig. 6. In this scenario, the input current will be introduced by $\langle \dot{Q}_0^L \rangle$, where $Q_0^L = C_g(\dot{\phi}_0^R - \dot{\phi}_0^L)$, for a given state that satisfies $\langle \dot{Q}_0^L \rangle = I_0 \sin(\Omega t)$. The Lagrangian describing this system is

$$\begin{aligned} \mathcal{L} = & \sum_{i=1}^{\infty} \left[\frac{\Delta x C_0}{2} (\dot{\phi}_i^L)^2 - \frac{(\phi_i^L - \phi_{i+1}^L)^2}{2\Delta x L_0} \right] - \frac{(\phi_0^L - \phi_1^L)^2}{2\Delta x L_0} \\ & + \frac{C_g}{2} (\dot{\phi}_0^R - \dot{\phi}_0^L)^2 + \frac{C_c}{2} (\dot{\phi}_0^R)^2 - \frac{(\phi_1^R - \phi_0^R)^2}{2\Delta x' L_1} \\ & + \sum_{j=1}^{\infty} \left[\frac{\Delta x' C_1}{2} (\dot{\phi}_j^R - V_0)^2 - \frac{(\phi_{j+1}^R - \phi_j^R)^2}{2\Delta x' L_1} \right], \end{aligned} \quad (25)$$

where now the capacitance and inductance corresponding to the left transmission line are C_0 and L_0 , and the ones corresponding to the right transmission line are C_1 and L_1 . The Euler-Lagrange equations for ϕ_0^L and ϕ_0^R are

$$C_g(\ddot{\phi}_0^L - \ddot{\phi}_0^R) = \frac{2\dot{\phi}_{in}^L(t)}{Z_0} - \frac{\dot{\phi}_0^L}{Z_0}, \quad (26)$$

$$C_g(\ddot{\phi}_0^R - \ddot{\phi}_0^L) + C_c \ddot{\phi}_0^R = \frac{2\dot{\phi}_{in}^R(t)}{Z_1} - \frac{\dot{\phi}_0^R}{Z_1}, \quad (27)$$

since the wave equation is satisfied inside each of the transmission lines for a flux field. Z_0 is the impedance on the left transmission line, and Z_1 the one on the right transmission line. We use the Euler-Lagrange equations to find expression for the outgoing modes in terms of the ingoing ones,

$$\begin{aligned} a_{out}^L(\omega) &= a_{in}^L(\omega) R_0(\omega) + a_{in}^R(\omega) s(\omega), \\ a_{out}^R(\omega) &= a_{in}^R(\omega) R_1(\omega) + a_{in}^L(\omega) s(\omega), \end{aligned} \quad (28)$$

at both sides of the system. In this circuit, the modes of the source, i.e. the transmission line on the left, are also reflected. The reflection coefficients are given by

$$\begin{aligned} R_0(\omega) &= \frac{1 - i\omega(C_g + C_c)Z_1 + \omega C_g Z_0(i + \omega C_c Z_1)}{1 - i\omega(C_g + C_c)Z_1 - \omega C_g Z_0(i + \omega C_c Z_1)}, \\ R_1(\omega) &= \frac{1 + i\omega(C_g + C_c)Z_1 - \omega C_g Z_0(i + \omega C_c Z_1)}{1 - i\omega(C_g + C_c)Z_1 - \omega C_g Z_0(i + \omega C_c Z_1)}, \end{aligned} \quad (29)$$

and the transmission coefficient is defined as

$$s(\omega) = \frac{-2i\omega C_g \sqrt{Z_0 Z_1}}{1 - i\omega(C_g + C_c)Z_1 - \omega C_g Z_0(i + \omega C_c Z_1)}. \quad (30)$$

Averaging over the vacuum state of the right transmission line, we write the voltage response of the circuit for a given state for the source

$$\begin{aligned} \langle \dot{\phi}_0^R \rangle = & -C_g Z_1 \sqrt{\frac{\hbar Z_0}{4\pi}} \int_0^\infty d\omega \omega^{3/2} \left\{ \frac{(1 - \omega^2 C_g C_c Z_0 Z_1) (\langle a_{\text{in}}^L(\omega) \rangle e^{-i\omega t} + \langle a_{\text{in}}^{L\dagger}(\omega) \rangle e^{i\omega t})}{1 + \omega^2 (C_g^2 Z_0^2 + 2C_g^2 Z_0 Z_1 + ((C_c + C_g)^2 + \omega^2 C_g^2 C_c^2 Z_0^2) Z_1^2)} \right. \\ & \left. + \frac{i\omega ((C_c + C_g) Z_1 + C_g Z_0) (\langle a_{\text{in}}^L(\omega) \rangle e^{-i\omega t} - \langle a_{\text{in}}^{L\dagger}(\omega) \rangle e^{i\omega t})}{1 + \omega^2 (C_g^2 Z_0^2 + 2C_g^2 Z_0 Z_1 + ((C_c + C_g)^2 + \omega^2 C_g^2 C_c^2 Z_0^2) Z_1^2)} \right\}. \end{aligned} \quad (31)$$

Computing the second moment of the voltage, we find

$$\begin{aligned} \langle (\dot{\phi}_0^R)^2 \rangle = & \frac{\hbar Z_1}{\pi} \int_0^\infty d\omega \frac{\omega(1 + \omega^2 C_g^2 Z_0^2)}{1 + \omega^2 (C_g^2 Z_0^2 + 2C_g^2 Z_0 Z_1 + ((C_c + C_g)^2 + \omega^2 C_g^2 C_c^2 Z_0^2) Z_1^2)} \\ & - \frac{\hbar Z_1}{4\pi} \int d\omega d\omega' \sqrt{\omega\omega'} \left\{ \langle a_{\text{in}}^L(\omega) a_{\text{in}}^L(\omega') \rangle s(\omega) s(\omega') e^{-i(\omega+\omega')t} - \langle a_{\text{in}}^L(\omega) a_{\text{in}}^{L\dagger}(\omega') \rangle s(\omega) s^*(\omega') e^{-i(\omega-\omega')t} \right. \\ & \left. - \langle a_{\text{in}}^{L\dagger}(\omega) a_{\text{in}}^L(\omega') \rangle s^*(\omega) s(\omega') e^{i(\omega-\omega')t} + \langle a_{\text{in}}^{L\dagger}(\omega) a_{\text{in}}^{L\dagger}(\omega') \rangle s^*(\omega) s^*(\omega') e^{i(\omega+\omega')t} \right\}, \end{aligned} \quad (32)$$

where the first term is again related to the reflection of the modes on the circuit, and it is purely quantum. The second term gives the frequency correlations of the modes on the left transmission line. For different dependencies of the circuit voltage on Z_0 , we solve Eq. 24 numerically to obtain the impedance of the memristor. Then, we compute the potassium channel conductance and the membrane voltage. This is equivalent, as mentioned above, to a strong adiabatic approximation, in which the impedance is considered constant in order to update the voltage of the circuit.

IV. RESULTS

In this section, we present the results of the membrane voltage and the potassium channel conductance for the single-ion channel Hodgkin-Huxley model. This is done by solving Eq. 24 for the update of the impedance of the memristor using each of the results of the membrane voltage given by the different inputs. We introduce the solutions of membrane voltage and ion channel conductances for the complete Hodgkin-Huxley model with a classical AC current source, which we use to compare with the single-channel Hodgkin-Huxley model. Then we show the results of the simulation for the quantized Hodgkin-Huxley model with a classical AC current source, and compare with the classical model. In each case we find that the potassium conductance reproduces the s-shaped curve as found in [1], with an initial offset of the rise leading to an eventual relaxation, meaning an adaptation to the input signal.

A. Classical Hodgkin-Huxley model

The complete Hodgkin-Huxley model with an AC current source is simulated by solving the Hodgkin-Huxley equations, i.e. Eqs. 1 - 4. Then, we plot in Fig. 7 the membrane voltage, the potassium channel

conductance, and the sodium channel conductance. This includes the correction given by the leakage channel, for a periodic input of the form $I(t) = I_0 \sin(\Omega t)$. The sodium conductance is included as $g_{Na} = \bar{g}_{Na} m^3 h$, and the conductance of the leakage channel is assumed constant, $g_L = \bar{g}_L$. For the membrane voltage taken to be initially zero, we plot it versus time in Fig. 7 (a) as the blue curve. The red curve in Fig. 7 (a) corresponds to the potassium channel conductance, and the curve in Fig. 7 (b) represents the sodium channel conductance.

A spike in the membrane voltage can be observed, with a subsequent decrease and adaptation to the input, leading to oscillations around the zero value. This is because we have taken the resting membrane voltage to be zero initially, and have set $V_K = 0$, where normally it is taken to be $V_K = -77\text{mV}$. We have chosen this according with the results for the response of the quantized model, in which this classical DC voltage source does not appear. In principle, this does not change the dynamical behavior, it just gives a displacement of the voltage. In fact, the profile of the voltage, aside from the oscillations caused by our choice of input current, accurately fits the plots depicted in Ref. [1].

The potassium conductance features rising and adaptive behavior. The sodium conductance is reproduced with great accuracy according to Ref. [1], with a clear spike and a slow relaxation that eventually features oscillations. We can observe that, with the displacement of the membrane potential, the sodium activation channels switches on fast resulting in a spike in the conductance. Then, when potassium ions leave the axon in order to offset the increase of positive charge inside it, inactivation is switched on, and sodium ions gradually leave the cell.

We use these results to contrast with the single-ion channel Hodgkin-Huxley model, finding that the behavior of the membrane voltage and the potassium channel

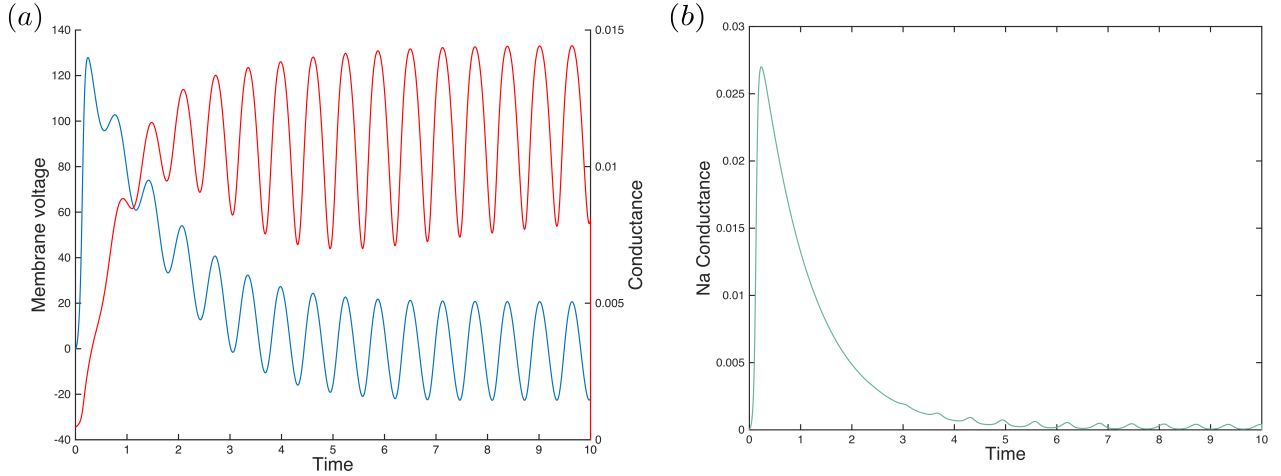


FIG. 7. Complete Hodgkin-Huxley model featuring potassium, sodium, and leakage channels with a periodic input $I(t) = I_0 \sin(\Omega t)$: (a) Membrane voltage (blue) and potassium channel conductance (red) over time. (b) Sodium channel conductance versus time.

conductance still feature the main characteristics of the complete Hodgkin-Huxley model. The solutions presented below correspond to the classical single-ion channel Hodgkin-Huxley model with a classical AC current source. Solving Eqs. 5 and 6, the resulting membrane voltage with a periodic input current of the form $I(t) = I_0 \sin(\Omega t)$, when taking the membrane voltage to be initially zero, can be seen plotted over time as the blue curve in Fig. 9 (a).

We can observe an initial spike in the voltage, followed by a recoil and an eventual adaptation, in which the voltage oscillates around zero. It is interesting to see that the spiking behavior of the membrane voltage can be reproduced in this simplified model featuring only potassium conductance. As the values for the coefficients $\alpha(V_g)$ and $\beta(V_g)$ were obtained through comparison with experimental results [1], the gate-opening probabilities may not be completely independent, so the mechanism of each ion channel cannot be isolated, as the transmission of the nervous impulse is a balanced process involving (in this case, two) different ion permeability changes.

Comparing the conductance as the red curve in Fig. 9 (b) with the ones obtained in Ref. [1], we see an initial delay of the increase with an eventual relaxation. It can be appreciated that with the introduction of an input signal the conductance rises and adapts to this signal, according to the depolarization of the membrane, with oscillations caused by our choice of $I(t)$. The I-V characteristic curve plotted in Fig. 8 displays a hysteresis loop which forms a limit cycle due to the periodic driving of the system when the system saturates.

When we solve the quantized Hodgkin-Huxley model, we use an adiabatic approximation. In order to fairly

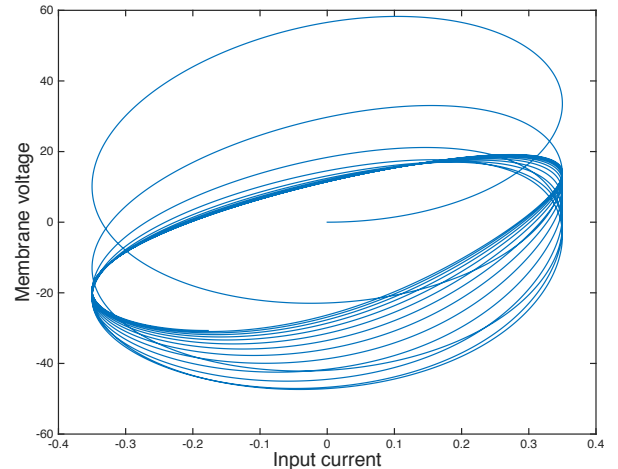


FIG. 8. Membrane voltage versus input current corresponding to the classical Hodgkin-Huxley model with a single ion channel subjected to an input current $I(t) = I_0 \sin(\Omega t)$.

compare the classical and quantized models, we need to study the classical Hodgkin-Huxley model with an adiabatic approximation.

In this case we have that the potassium conductance is given by $g_K = \bar{g}_K n^4(t)$, so when solving Eqs. 5 and 6 we take $n(t)$ to be constant, which allows for a straightforward solution of $V_g(t)$, with the choice of $I(t) = I_0 \sin(\Omega t)$,

$$V_g(t) = V_K + I_0 \frac{g_K \sin(\Omega t) - \Omega C_m \cos(\Omega t)}{g_K^2 + C_m^2 \Omega^2}, \quad (33)$$

where we have only considered the stationary solution, given that the transitory one provides fast decay.

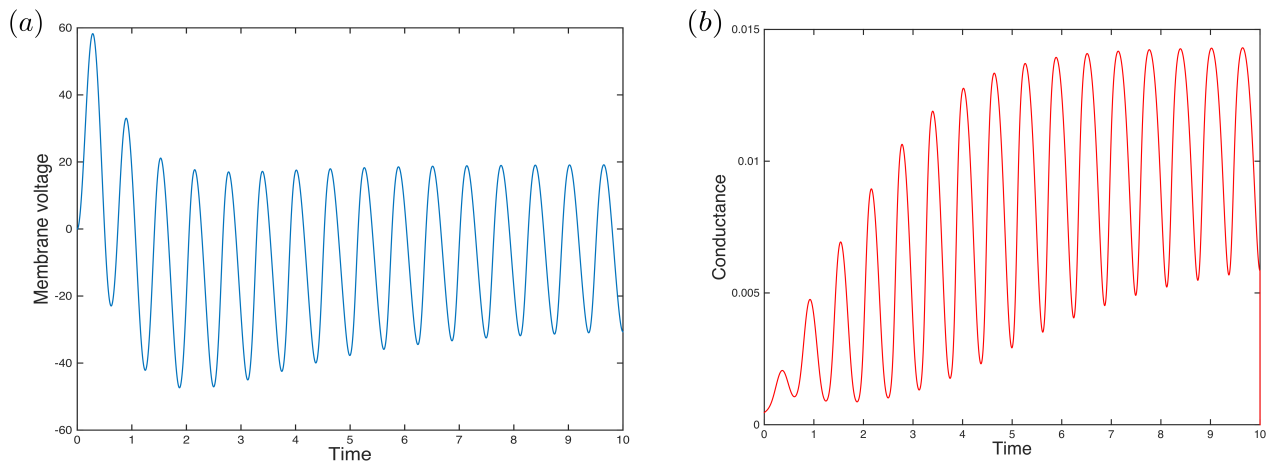


FIG. 9. Classical Hodgkin-Huxley model for a single ion channel with a periodic input $I(t) = I_0 \sin(\Omega t)$: (a) Membrane voltage over time. (b) Potassium channel conductance over time.

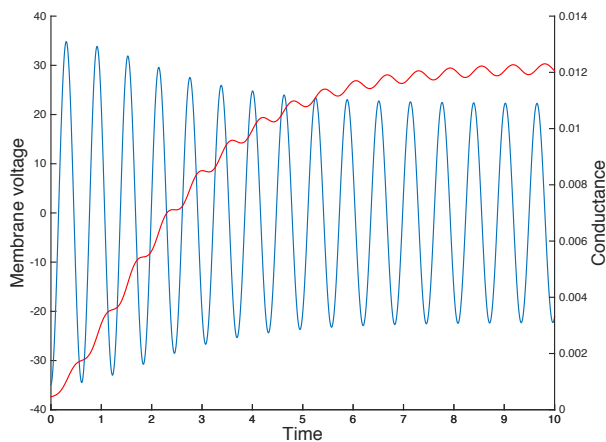


FIG. 10. Membrane voltage (blue) and potassium channel conductance (red) over time in the classical Hodgkin-Huxley model with a periodic input $I(t) = I_0 \sin(\Omega t)$ solved by using an adiabatic approximation.

Using this result, we solve for $n(t)$ at any time step, and plot the results of the membrane voltage and the potassium channel conductance in Fig. 10,

B. Quantum Hodgkin-Huxley model

The simulation of the quantum Hodgkin-Huxley model uses a classical AC current source, and the solutions for the membrane voltage, the potassium channel conductance and the characteristic I-V curve are presented here. By solving Eqs. 21 and 24, we obtain the membrane voltage and the potassium conductance in the quantum model with a classical input $I(t) = I_0 \sin(\Omega t)$. The membrane voltage against time is plotted as the blue curve in Fig. 11 (a). We observe no interesting

dynamics, but rather a decrease in amplitude and a relaxation of the oscillations as it adapts to the input.

The conductance in Fig. 11 (a) (red curve) does not feature the desired delay in its growth, but its saturation is more clear, and although it saturates faster, it starts to resemble the desired s-shaped curve displayed by the saturation of the potassium conductance in Ref. [1].

We can see that the membrane voltage and the potassium channel conductance plotted in Fig. 11 (a) are the same as depicted in Fig. 10, meaning that the response to a classical input source in the quantum regime is the same as in the classical one with an adiabatic approximation.

We introduce the I-V characteristic curve as we plot the membrane voltage versus the input current, shown in Fig. 11 (b), featuring a memristive hysteresis loop. The shape of this curve depends on the initial conditions, as initial values further away from the maximal value of the impedance will cause the system to have a longer saturation time. However, the system eventually relaxes into a limit cycle, whose shape is independent of the initial conditions.

The area of the hysteresis loop can give us a hint about the memory persistence in the system [18, 19], such that the larger the area, the greater the memory persistence. Then, it would be interesting to test whether the introduction of a quantized Hodgkin-Huxley model that allows for the use of quantum state inputs represents an improvement in the persistence of the memory or not. Particularly, entangled states are the desired states for this test. The information carried out by quantum states can be related to classical information through Landauer's principle, being classical dissipation the link, where the area of the hysteresis loop intervenes.

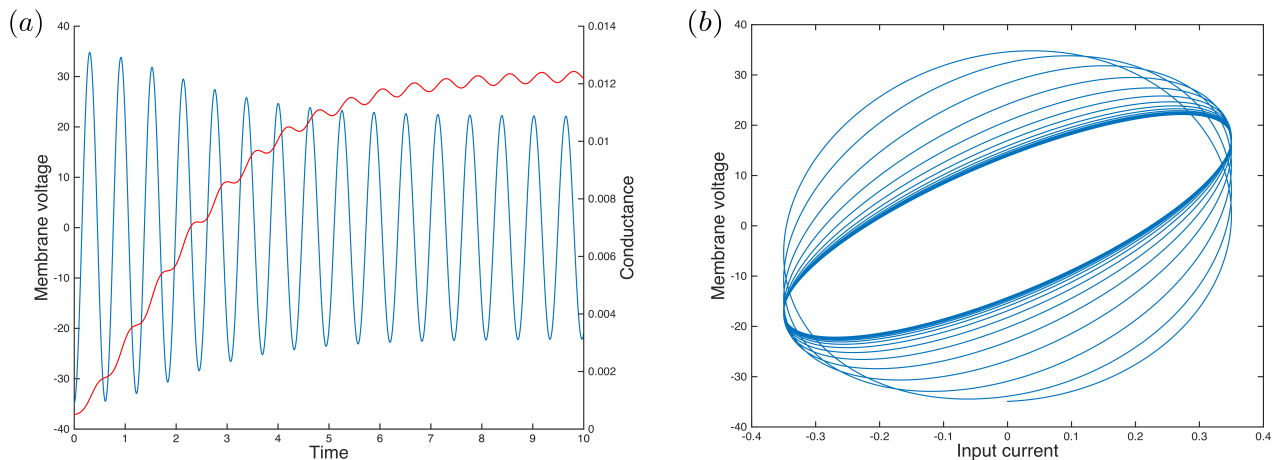


FIG. 11. Quantum Hodgkin-Huxley model with a classical periodic input $I(t) = I_0 \sin(\Omega t)$: (a) Membrane voltage (blue) and potassium conductance (red) over time. (b) Membrane voltage versus input current.

V. CONCLUSIONS & OUTLOOK

We have studied a simplified version of the Hodgkin-Huxley model with a single ion channel as a circuit featuring a capacitance, a voltage source and a memristor under a periodic input both in the classical regime, and in the quantum regime by introducing a quantum memristor. Then, we compared the membrane voltage, the potassium conductance and the I-V characteristic curve in both regimes.

This work shows that the behavior of this simplified version of the classical Hodgkin-Huxley model can be reproduced in the quantum regime, with the spike in the membrane voltage replaced by a slow relaxation. The voltage response of the circuit is found to be classical, but the second moment actually features a quantum term given by how the modes are reflected in the circuit. The conductance is in good accordance with the experiments carried out in Ref. [1], rising as a s-shaped curve. This is a result of a displacement from a resting value by an input source with an eventual adaptation, unaffected by intermediate and relaxation oscillations. This saturation or adaptation is identified with a learning process by the memristive device.

Beyond this simplified model, a study of the two-ion channel Hodgkin-Huxley model in the quantum regime, which amounts to adding a second memristor corresponding to the conductance of the sodium channel, would unveil new characteristics of the mechanism that rules the conduction of nervous impulses in neurons. For example, we expect to see an initial spike in the sodium conductance, knowing that the mechanism of the sodium channel consists of a fast activation gate followed by inactivation. But this work would also carry

a complete new result of a different kind: the dynamics of two quantum memristors connected in parallel have never been studied.

Another interesting line to follow is to study the effects of quantum state inputs on the system, where memory effects are revealed by the area of the hysteresis loop. However, memory effects are more relevant when displayed in connected neuron networks, by studying, for example, the output of a string of neurons with an entangled state input, which would imply yet another novel discovery: the dynamics of two serially-connected circuits featuring quantum memristors have never been studied either.

A study of the dynamics of coupled quantum memristors based on recent works in serial and parallel coupled memristor circuits [20–22] can give an answer to these two questions, which would set excellent starting points for any advances in neuromorphic quantum computing and quantum neural networks, with direct applications on quantum machine learning.

ACKNOWLEDGEMENT

The authors acknowledge support from NSFC (11474193), the Shuguang (14SG35), the program of Shanghai Municipal Science and Technology Commission (18010500400 and 18ZR1415500), Spanish MINECO/FEDER FIS2015-69983-P and Basque Government IT986-16. The authors also acknowledge support from the projects QMiCS (820505) and OpenSuperQ (820363) of the EU Flagship on Quantum Technologies. This material is also based upon work supported by the U.S. Department of Energy, Office of Science, Office of Advance Scientific Computing Research (ASCR), under field work proposal number ERKJ335.

-
- [1] A. L. Hodgkin and A. F. Huxley, “A quantitative description of membrane current and its application to conduction and excitation in nerve”, *J. Physiol.* **117**, 500 (1952).
- [2] S.-G. Lee, A. Neiman, and S. Kim, “Coherence resonance in a Hodgkin-Huxley neuron”, *Phys. Rev. E* **57**, 3292 (1998).
- [3] Y.-Q. Wang, David T. W. Chik, and Z. D. Wang, “Coherence resonance and noise-induced synchronization in globally coupled Hodgkin-Huxley neurons”, *Phys. Rev. E* **61**, 740 (2000).
- [4] C. Zhou and J. Kurths, “Noise-induced synchronization and coherence resonance of a Hodgkin-Huxley model of thermally sensitive neurons”, *Chaos* **13**, 401 (2003).
- [5] L. A. da Silva and R. D. Vilela, “Colored noise and memory effects on formal spiking neuron models”, *Phys. Rev. E* **91**, 062702 (2015).
- [6] E. Yilmaza, V. Baysala, and M. Ozer, “Enhancement of temporal coherence via time-periodic coupling strength in a scale-free network of stochastic Hodgkin-Huxley neurons”, *Phys. Lett. A* **379**, 1594 (2015).
- [7] X.-M. Guo, J. Wang, J. Liu, H.-T. Yu, and R. F. Galán, “Optimal time scales of input fluctuations for spiking coherence and reliability in stochastic Hodgkin-Huxley neurons”, *Physica A* **468**, 381 (2017).
- [8] H.-T. Yu, R. F. Galán, J. Wang, Y.-B. Cao, and J. Liu, “Stochastic resonance, coherence resonance, and spike timing reliability of Hodgkin-Huxley neurons with ion-channel noise”, *Physica A* **471**, 263 (2017).
- [9] Y.-H. Hao, Y.-B. Gong, X. Lin, Y.-H. Xie, and X.-G. Ma, “Transition and enhancement of synchronization by time delays in stochastic Hodgkin-Huxley neuron networks”, *Neurocomputing*, **73**, 2998 (2010).
- [10] L. O. Chua, “Memristor-The missing circuit element”, *IEEE Trans. Circuit Theory* **18**, 507 (1971).
- [11] L. O. Chua and S. M. Kang, “Memristive devices and systems”, *Proc. IEEE* **64**, 209 (1976).
- [12] M. Mohseni, P. Rebentrost, S. Lloyd, and A. Aspuru-Guzik, “Environment-assisted quantum walks in photosynthetic energy transfer”, *J. Chem. Phys.* **129**, 174106 (2008).
- [13] M. Mohseni, Y. Omar, G. S. Engel, and M. B. Plenio, *Quantum effects in biology*, (Cambridge University Press, Cambridge, 2014).
- [14] U. Alvarez-Rodriguez, M. Sanz, L. Lamata, and E. Solano, “Artificial Life in Quantum Technologies”, *Sci. Rep.* **6**, 20956 (2016)
- [15] U. Alvarez-Rodriguez, M. Sanz, L. Lamata, and E. Solano, “Quantum Artificial Life in an IBM Quantum Computer”, *Sci. Rep.* **8** 14793 (2018).
- [16] U. Alvarez-Rodriguez, M. Sanz, L. Lamata, and E. Solano, “Biomimetic Cloning of Quantum Observables”, *Sci. Rep.* **4**, 4910 (2014)
- [17] P. Pfeiffer, I. L. Egusquiza, M. Di Ventra, M. Sanz, and E. Solano, “Quantum Memristor”, *Sci. Rep.* **6**, 29507 (2016).
- [18] J. Salmilehto, F. Deppe, M. Di Ventra, M. Sanz, and E. Solano, “Quantum Memristors with Superconducting Circuits”, *Sci. Rep.* **7**, 42044 (2017).
- [19] M. Sanz, L. Lamata, and E. Solano, “Quantum Memristors in Quantum Photonics”, *APL Photonics* **3**, 080801 (2018).
- [20] D. Yu, H. H.-C. Iu, Y. Liang, T. Fernando, and L. O. Chua, “Dynamic Behavior of Coupled Memristor Circuits”, *IEEE Trans. Circuits and Systems I* **62**, 1607 (2015).
- [21] R. K. Budhathoki, M. Pd. Sah, S. P. Adhikari, H. Kim, and L. O. Chua, “Composite Behavior of Multiple Memristor Circuits”, *IEEE Trans. Circuits and Systems I* **60**, 2688 (2013).
- [22] L. O. Chua, “Resistance Switching Memories are Memristors”, *Applied Physics A* **102**, 765 (2011).
- [23] N. Gomez, J. O. Winter, F. Shieh, A. E. Saunders, B. A. Korgel, and C. E. Schmidt, “Challenges in quantum dot-neuron active interfacing”, *Talanta*, **67**, 462 (2005).
- [24] M. Maeda, M. Suenaga, and H. Miyajima, “Qubit neuron according to quantum circuit for XOR problem”, *Appl. Math. Comput.* **185**, 1015 (2007).
- [25] Michail Zak, “From quantum entanglement to mirror neuron”, *Chaos*, **34**, 344 (2007).
- [26] D. Ventura and T. Martinez, *An Artificial Neuron with Quantum Mechanical Properties*, (Springer, Vienna, 1998), pp. 482-485.
- [27] Y. Cao, G. G. Guerreschi, and A. Aspuru-Guzik, “Quantum Neuron: an elementary building block for machine learning on quantum computers”, arXiv: 1711.11240 (2017).
- [28] N. Kouda, N. Matsui, and H. Nishimura, “Learning performance of neuron model based on quantum superposition”, *IEEE RO-MAN*, 112 (2000).
- [29] G. S. Snider *et al.*, “From synapses to circuitry: Using memristive memory to explore the electronic brain”, *Computer* **44**, 21 (2011).
- [30] R. Berdan, E. Vasilaki, A. Khiat, G. Indiveri, A. Serb, and T. Prodromakis, “Emulating short-term synaptic-dynamics with memristive devices”, *Sci. Rep.* **6**, 18639 (2015).
- [31] Y. V. Pershin and M. Di Ventra, “Neuromorphic, Digital, and Quantum Computation with Memory Circuit Elements”, *Proc. IEEE* **100**, 2071-2080 (2012).
- [32] T. Serrano-Gotarredona, T. Masquelier, T. Prodromakis, G. Indiveri, and B. Linares-Barranco, “STDP and STDP variations with memristors for spiking neuromorphic learning systems”, *Front. Neurosci.* **7**, 2 (2013).
- [33] T. Gonzalez-Raya, Master Thesis: *Quantized Hodgkin-Huxley Model for Quantum Neurons*, (Universidad del Pais Vasco, 2018).
- [34] F. Silva, M. Sanz, J. Seixas, E. Solano, and Y. Omar, “Perceptrons from Memristors”, arXiv: 1807.04912 (2018).
- [35] M. Schuld, I. Sinayskiy, and F. Petruccione, “An introduction to quantum machine learning”, *Contemp. Phys.* **56**, 172 (2015).
- [36] J. Biamonte, P. Wittek, N. Pancotti, P. Rebentrost, N. Wiebe, and S. Lloyd, “Quantum Machine Learning”, *Nature* **549**, 195 (2017).
- [37] G. Z. Cohen, Y. V. Pershin, and M. Di Ventra, “Lagrange Formalism of Memory Circuit Elements: Classical and Quantum Formulation”, *Phys. Rev. B* **85**, 165428 (2012).
- [38] U. Vool and M. Devoret, “Introduction to Quantum Electromagnetic Circuits”, *Int. J. Circuit Theory and Applications* **45**, 897 (2016).

- [39] M. Sanz, E. Solano, and I. L. Egusquiza, *Beyond Adiabatic Elimination: Effective Hamiltonians and Singular Perturbation*, (Springer, Japan, 2016), pp. 127-142.
- [40] B. Yurke and J. S. Denker, “Quantum Network Theory”, *Phys. Rev. A* **29**, 1419 (1984).